Paste 2026 – AB Fourie, M Horta, M Oliveira & S Wilson (eds)

doi:10.36487/ACG_repo/2655_53

Reducing water consumption by online measuring of rheology using a pipe rheometer

Bas Nieuwboer [a,*], Arno Talmon [b], Gustavo Hamú [a]

[a] *IHC Mining, Netherlands*

[b] *Delft University of Technology, Netherlands*

Abstract

Due to the shortage of freshwater, identifying strategies to reduce water consumption in mining areas has become crucial.

One of the primary methods employed to reduce water consumption is the use of tailings thickeners, which promote the settling of suspended solids and allows water to be recovered and reused within the process plant, thereby reducing the need for external freshwater sources. Transporting thicker tailings will result in water savings at the cost of an increased pressure loss in pipeline transport.

However, control of these thickeners based on solids content measurements or density measurements alone has been proven insufficient, making rheology measurements necessary. Yet, manual rheology measurements do not provide sufficient information for the control system, due to the low measuring frequency – most often once or twice a day. The autonomous rheology meter (ARM), a pipe rheometer, addresses this limitation by measuring rheology every 15 min, providing real-time values for Bingham yield stress and plastic viscosity.

By providing, high-frequency rheological data, the ARM enables operators to safely reduce the water content in tailings while ensuring that the slurry remains transportable without risking pipeline blockage.

The working principle of the ARM is based on measuring the pressure differences in a U-loop. This results in a wall-shear stress, which is used to compute the yield stress and Bingham viscosity. This paper compares these results against a conventional Haake roto-viscometer laboratory test.

Additionally, possible water savings will be estimated, based on the theoretical, calibrated and validated relationship between water content to fines ratio and rheological parameters for tailings. From the water content to fines ratio, the mixture density can be computed, as well as the energy required for hydraulic transport.

Keywords: *autonomous rheology meter, water savings*

1 Introduction

Globally, freshwater is scarce and mining operations require a lot of water to extract the valuable minerals. The mining sites are generally located in remote arid regions. Water recovery is therefore of a great importance resulting in a lesser use of freshwater and simplifying the storage of the tailings in tailing ponds.

Tailing thickeners recover the water from the tailings. In the thickener, suspended solids settle and the water is returned to the process plant. Water recovery has a downside, it increases the density and yield stress of the tailings, enhancing the wall friction of the tailings during transportation. When the friction is higher than the pressure delivered by the pump, the pipeline will get clogged. To assure the pipeline does not get clogged,

* Corresponding author. Email address: B.J.Nieuwboer@royalIHC.com

the density, yield stress and the Bingham viscosity should be limited. Therefore, these parameters are measured frequently.

Usually, the rheology (yield stress and Bingham viscosity) is measured daily or bi-daily by taking a sample, whereafter it is sent to the laboratory for analysis. The yield stresses of copper tailings presented in van Wijk et al. (2023) show a variability of 20–60 Pa. In-between measurements operators have to account for the variability in the yield stress and density by taking a safety margin on the thickening process. This ensures that when the tailings have a higher density and yield stress in-between the measurements, they will still be transported and the pipeline won't get clogged.

Many authors aim at water savings in the mining industry. This paper shows a method for continuously measuring the rheology, enabling a safe operation when reducing the water content in the tailings. The autonomous rheology meter (ARM) is designed to measure the rheology and density of tailings every 15 min. Using this information the tailings thickener can be optimised to recover more water. In addition, the ARM can be used at all locations where more frequent measurements of the rheology are beneficial to save water.

This paper will show the ARM, its working principle and results from measurements at the Royal IHC yard using a clay mixture. The method for computing the water savings and the resulting energy consumption will also be outlined. This water savings and energy consumption has been computed for 4 tailings from literature.

2 Autonomous rheology meter

The measurement of the rheology of the tailings is performed using a pipe rheometer, which can be placed downstream of a tailings thickener to manually adjust the thickener for higher water extraction. Part of the tailings is diverted to the ARM, whereafter, the ARM draws in slurry via an inlet pipe to the pump. This pump directs the flow through a U-loop, as shown in Figure 1. The flow velocities in the pipes are controlled by opening or closing pinch valves that are situated after the U-loop. The measurement data is gathered from the system in cycles of 15 min. This data is processed and a new datasheet with rheology information is produced.

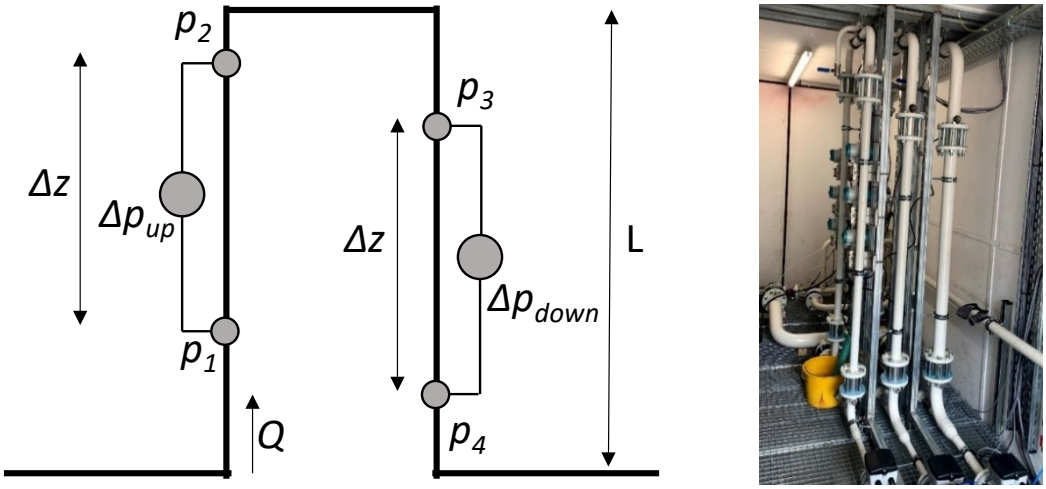

Figure 1 Schematic representation and a photo of the U-loop in the autonomous rheology meter

To allow for easy transport of the ARM, it is set up in a standard 20 ft container (standard 20 ft high cube), that can be shipped using standard shipping methods. This container contains the complete system with piping, pumps, sensors, control cabinet and visualisation on a touch screen. It has 2 inlet and 2 outlet flanges for both a tailings and flush-water line in and output. The ARM is powered using a CEE32A plug with 400 V AC~3 / 50 Hz.

Other pipe rheometers have been presented in the literature. Van Wijk et al. (2023) gives an overview of these pipe rheometers. Chryss et al. (2019) presented a horizontal pipe rheometer based on the same principle as the ARM. However, in a horizontal measurement section coarse particles can settle down,

influencing the measured pressure to drop over the section. Gruszczyński et al. (2022) presented a U-loop for measuring the density of dredged tailings in a copper tailings pond; however, they did not measure the rheological parameters.

2.1 Working principle

van Wijk et al. (2023) and Talmon et al. (2024) describe the working method of the ARM, which uses the U-loop principle based on Clift & Manning-Clift (1981). In the U-loop the discharge and the pressure difference in the vertical up and down sections is measured. Equation 1 shows the pressure difference in the riser and downcomer sections. These equations assume a steady state flow in the U-loop, and an equal density and wall shear stress in both sections.

$$\Delta p_{up} = \rho_m \, g \, \Delta z + \frac{4 \, \tau_w \, \Delta z}{D} \qquad \Delta p_{down} = -\rho_m \, g \, \Delta z + \frac{4 \, \tau_w \, \Delta z}{D} \tag{1}$$

where:

Δp_{up} and Δp_{down} = the pressure differences in each section, respectively (Pa)

ρ_m = the mixture density (kg/m^3)

g = the gravitational constant (m/s^2)

Δz = the spacing between the sensors (m)

D = the pipe diameter (m)

τ_w = the wall shear stress in each leg (Pa).

From the 2 relations shown in Equation 1, the pressure, the wall shear stress and the density can be computed:

$$\tau_w = D \frac{\Delta p_{up} + \Delta p_{down}}{8 \, \Delta z} \qquad \rho_m = \frac{\Delta p_{up} - \Delta p_{down}}{2 \, g \, \Delta z} \tag{2}$$

In this paper we model the tailings as a Bingham fluid with a yield stress and a Bingham plastic viscosity:

$$\tau_w = \tau_y + \mu_B \, \dot{\gamma} \tag{3}$$

where:

τ_w = the wall shear stress (Pa)

τ_y = the yield stress (Pa)

μ_B = the Bingham plastic viscosity (Pa s)

$\dot{\gamma}$ = the shear rate (1/s).

The ARM uses 3 U-loops with different diameters for redundancy purposes and for the possibility of correcting wall slip in the measurement section (van Wijk et al. 2023). In all 3 U-loops the pressure differences and the discharge through the U-loops are measured. From this data and with use of Equation 2 the wall shear stress and tailings density is computed. From the wall shear stresses at a measured flow rate the Bingham parameters of Equation 3 are estimated by applying a non-linear Levenberg-Marquardt method to the Buckingham-Reiner equation (Equation 4) using the least squares method provided by the SciPy package in Python. This outputs the yield stress and Bingham viscosity with the smallest error between the measured data and the computed values.

$$Q = \frac{\pi}{\mu_B} \frac{\left(\tau_w - \tau_y\right)^2}{\left(\frac{\tau_w}{0.5\,D}\right)^3} \left[\frac{\left(\tau_w - \tau_y\right)^2}{4} + \frac{2\,\tau_y\left(\tau_w - \tau_y\right)}{3} + \frac{\tau_y^2}{2}\right] \tag{4}$$

where:

Q = the discharge through the U-loop (m^3/s).

The shear rate can be calculated based on the apparent shear rate using the Weissenberg–Rabinowitsch–Mooney relation:

$$\dot{\gamma} = \dot{\gamma}_a \left(\frac{3}{4} + \frac{1}{4}\frac{\mathrm{d}\ln\dot{\gamma}_a}{\mathrm{d}\ln\tau_w}\right) \tag{5}$$

where:

$\dot{\gamma}_a$ = the apparent shear rate defined as: $8\bar{u}/D$ (s^{-1})

$\bar{u}$ = is the average velocity over the cross-section of the pipe (m/s).

Magnon (2021) derived the derivative for a Herschel-Bulkley fluid. For a Bingham fluid this is:

$$\frac{\mathrm{d}\ln\dot{\gamma}_a}{\mathrm{d}\ln\tau_w} = \frac{\tau_w}{\tau_w - \tau_y} - \frac{4\,\tau_y\,\tau_w + 2\,\tau_y}{6\,\tau_w^2 + 4\,\tau_y\tau_w + 2\,\tau_y} - 1 \tag{6}$$

Using Equation 5 and 6 the shear rate can be computed based on the apparent shear rate.

2.2 Resulting rheology from measurements

At the IHC yard 2 main measurement campaigns were conducted in 2022 and 2024 using model tailings, a mixture of water with Sibelco FT-S1 clay consisting of 64% kaolinite group minerals, 10% sericite/illite and 19% quartz. Eighty-three percent of the particles are smaller than 2 µm. A 200 L tank, containing this mixture, was connected to the inlet of the ARM. The mixture was pumped back into the tank after going through the U-loops in the ARM.

In the 2022 measurement campaign we validated the method used in the ARM. One of the issues we encountered afterwards was the influence of temperature on the differential pressure measurements, which we aimed to resolve in the 2024 measurement campaign. Talmon et al. (2024) describe the 2024 measurement campaign and the temperature influence. They proposed a new sampling method with an additional density sensor. The differential pressure sensors were nulled every measurement cycle using the data of the density sensor when pumping the mixture, whilst the flow in the U-loop was zero. However, in case of zero flow, the clay mixture would hang in the pipe, under-estimating the differential pressure at the nulling procedure without any flow. It introduced an offset in the measurements. This showed that nulling the differential pressure sensors using a mixture with a yield stress will therefore introduce errors. Nulling should therefore be performed with water.

It is very likely that the offset in pressure differential measurement due to the temperature variation is far more pronounced in the lab setting where a very limited amount (200 L) of mixture is repeatedly pumped through the system. In a real-life situation, where the tailings are transported from a pond, the temperature of the tailings does not change much.

Figure 2 presents the data at 13:50 hours of the ARM compared to a flow curve of the Haake VT 550 roto-viscometer and shows the Bingham parameters computed by the ARM. Figure 3 present the outputted yield stress and the Bingham viscosity over the course of a workday. It shows that the yield stress is computed within 10% most of the time. The Bingham plastic viscosity has an error of 78% for the ARM data point at 13:50 hours (see lower panel of Figure 3). Whilst the error in Bingham plastic viscosity may seem large, the

apparent viscosity is a better measure of the ARM's performance. The apparent viscosity is the effective fluid viscosity at a specific shear rate and it is calculated by $\tau_w/\dot{\gamma}$ for the ARM measurement at 13:50. Figure 4 shows a small error (4.8%) in apparent viscosity at a shear rate of 400 s^{-1}, which is around highest shear rate measured by the ARM. At higher shear rates the error increases; however, this might be due to the lack of datapoints measured by the ARM. The highest errors are at the shear rates below 100 s^{-1}. This deviation is also visible in Figure 2 where the fit through the ARM data (black line) deviates from the Haake data (orange dots). Due to modelling the tailings as a Bingham fluid, thus only including a linear relation between the shear rate and shear stress, there will be an error in the model when the flow curve of the roto-viscometer is not linear. The apparent viscosity will not be outputted to the user of the ARM since it is complex for an operator to interpret. In this paper it is added for showing the small contribution of the Bingham plastic viscosity on the fluid property.

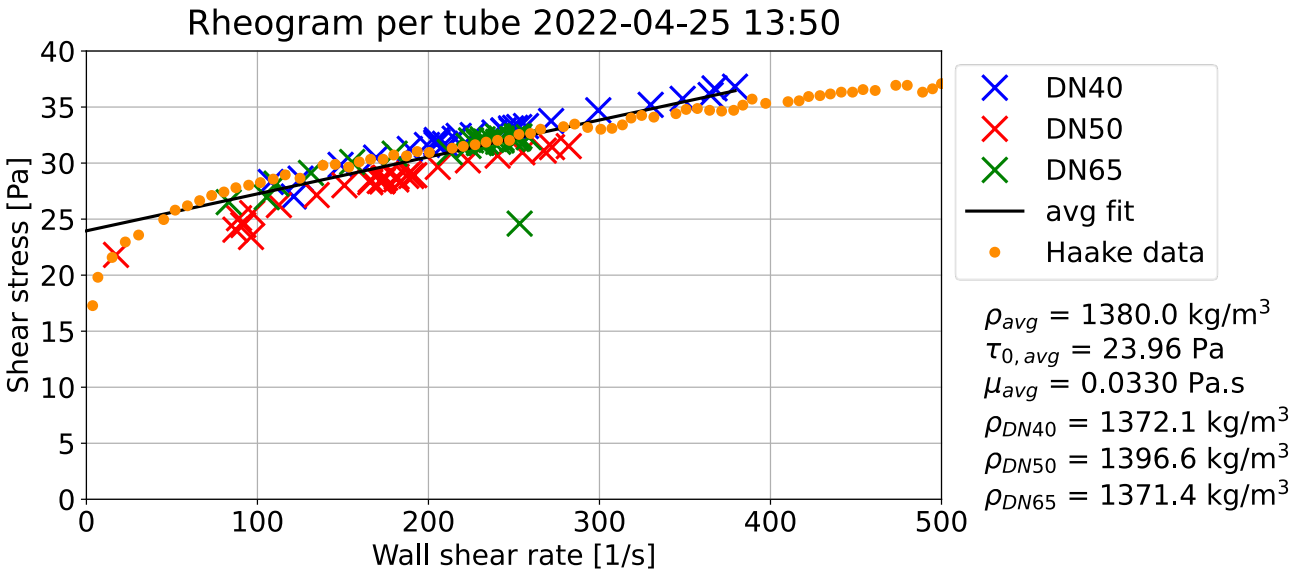

Figure 2 Rheogram measured using the autonomous rheology meter and compared to the Haake data from a sample taken at 13:52

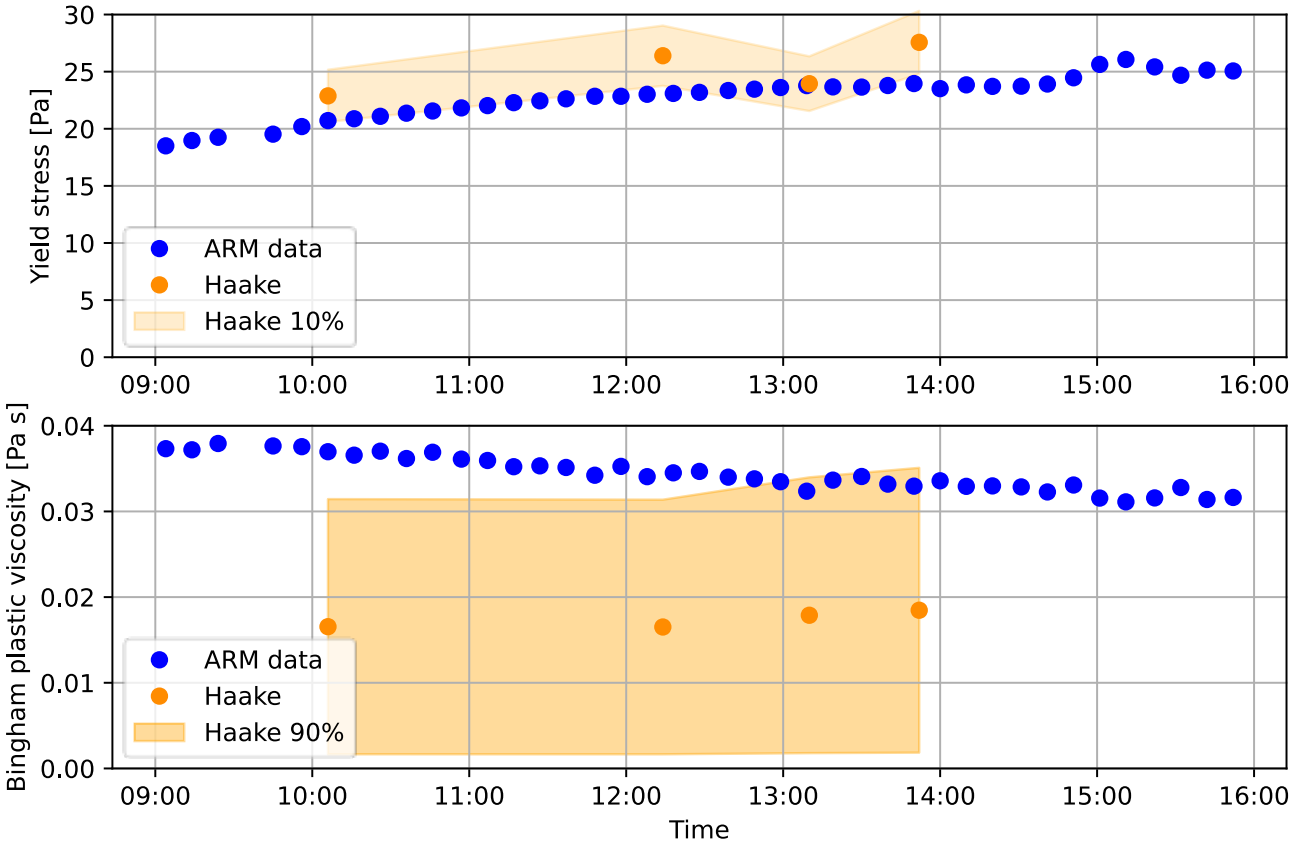

Figure 3 **Comparing the yield stress and Bingham plastic viscosity measured using the autonomous rheology meter (ARM) with the Haake measurements. The orange area indicates an error of 10% for the yield stress and a 90% error for the Bingham plastic data. Data from 25-04-2022**

Using the ARM's 3 U-loops, the error in measured density can be computed. This can act as indication to determine when to null the differential pressure sensors with clear water.

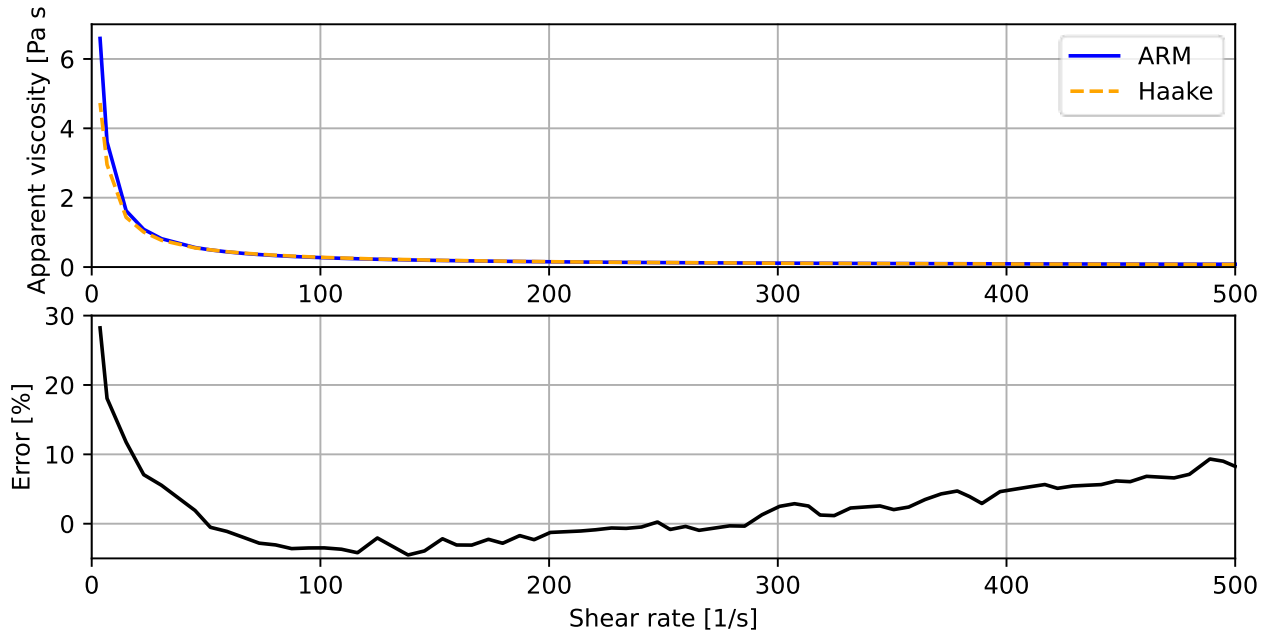

Figure 4 **Comparing the apparent viscosity measured by the autonomous rheology meter (ARM) with the Haake measurements (top). Error in the apparent viscosity between the ARM and Haake data (bottom). ARM data from 25-04-2022, 13:50**

3 Method for computing water savings

This paper present 4 data sets with different relations of yield stress to water content to fines ratios. We model this relation for each dataset, to compute both the water savings and the hydraulic gradient based on the yield stress. Riquelme (2020) shows a similar approach. The results of the model outline the amount of water that could be saved using the ARM.

3.1 Model for tailings and water savings

Jacobs et al. (2008) showed a fit for the yield stress and Bingham viscosity based on the water content to fines ratio (defined by Equation 8) and the linear concentration of the sand concentration in a claylike mixture, such as tailings. The model showed that the tailings are strengthened when more coarse particles are present. Data presented in Talmon et al. (2016) and van de Ree (2015) support this finding. Gruszczyński et al. (2019) presented another model based on the mass concentration. This data does not show a clear trend on the influence of sand in the tailings.

Sofrá & Boger (2011) presented a theory that the yield stress increases for finer particles in the slurry, since the particles have more surface area to interact with each other. From their illustration of mass concentration against yield stress for different amounts of sand, the same trend as in Jacobs et al. (2008) can be derived. In this study we use a simplified relation with the water content to fines ratio based on Jacobs et al. (2008):

$$\tau_y = K\, w_{cf}^{B} \tag{7}$$

where:

w_{cf} = the water content to fines ratio defined by Equation 8 (-)

K and B = dimensionless parameters.

The water content is defined as the weight of water over the weight of fines:

$$w_{cf} = \frac{w_{water}}{w_{fines}} \tag{8}$$

where:

w_{water} = the weight of the water in the tailings (kg)

w_{fines} = the weight of the fines (<74 μm) (kg).

Based on available data the 2 constants in Equation 5 can be evaluated for each specific tailing. The constants are determined using the Python SciPy curve fit method.

3.1.1 Water savings

The water savings in the tailings are a percentual decrease in water content to fines ratio (Equation 6), since the weight of the fines stays constant. The reduction of water in the tailings lead to an increase in yield stress as presented in Equation 7.

3.2 Hydraulic gradient

In computing the hydraulic gradient, we assume a constant transport of sediment (fines + sand) for each tailing. The hydraulic gradient is computed based on the Darcy friction factor f and the mixture density:

$$\frac{\mathrm{d}p}{\mathrm{d}x} = \frac{P}{A}\tau_w \qquad\qquad \tau_w = \frac{1}{8}\, f\, \rho_m\, \bar{u}^2 \tag{9}$$

where:

$\mathrm{d}p/\mathrm{d}x$ = the hydraulic gradient (pa/m)

P = the perimeter of the pipe (m)

A = the area of the pipe (m^2)

τ_w = the wall shear stress (Pa)

f = the Darcy friction factor (-)

ρ_m = the mixture density (kg/m^3).

3.2.1 Density and velocity

We assume a constant transport of sediment, which is dictated by the mine's production (Equation 10). An increase in concentration (and thus yield stress) therefore leads to a decrease in line speed (Equation 11).

$$Q_{solids} = c_v\, \bar{u} = \text{constant} \tag{10}$$

$$\bar{u} = \frac{c_{v,min}\, \bar{u}_{max}}{c_v} \tag{11}$$

where:

Q_{solids} = the volumetric solids transport (m^3/s)

$\bar{u}$ = the line speed at a given concentration (m/s)

c_v = the volumetric concentration at the computed line speed (-)

$\bar{u}_{max}$ = a maximum specified line speed (m/s)

$c_{v,min}$ = the minimum volumetric concentration at the maximum line speed (-).

The concentration of sand and fines is computed using Equation 8 and 12, where Equation 12 presents the sand to fine ratio (ratio):

$$SFR = \frac{w_{sand}}{w_{fines}} \tag{12}$$

where:

SFR = the Sand to Fine Ratio in the tailings (-)

w_{sand} = the weight of the sand in the tailing's fines (>74 µm) (kg].

For computing the hydraulic gradient, the density of the tailings is computed by:

$$\rho_m = c_v\, \rho_p + \, (1 - c_v)\, \rho_f \tag{13}$$

where:

ρ_f = the fluid density (kg/m^3)

ρ_p = the particle density (kg/m^3).

3.2.2 Friction factor

For a Bingham fluid the Darcy friction factor is computed in both the laminar and turbulent regime. In the laminar regime the friction factor can be computed using the dimensionless Buckingham-Reiner equation (Swamee & Aggarwal 2011):

$$f = \frac{64}{\mathrm{Re}}\left(1 + \frac{\mathrm{He}}{6\,\mathrm{Re}} - \frac{64}{3}\frac{\mathrm{He}^4}{f^3\,\mathrm{Re}^7}\right) \qquad \mathrm{Re} = \frac{\rho_m\,D\,\bar{u}}{\eta_B} \qquad \mathrm{He} = \frac{\rho_m\,D^2\,\tau_y}{\eta_B^2} \tag{14}$$

where:

Re = the Reynolds number (-)

He = the Hedström number (-)

D = the pipe diameter (m).

Note that this equation has to be solved implicitly since it is dependent on the friction factor itself. Swamee & Aggarwal (2011) presented a more practical friction factor which can be solved explicitly. However, since we have to solve the turbulent friction factor explicitly, we will use the exact dimensionless Buckingham-Reiner equation (Equation 14).

Many authors presented relations for the friction factor for turbulent Bingham flow. Dodge & Metzner (1959) is a well-known one. Yusufi et al. (2025) presented an overview of many relations. In this paper we will use the Wilson & Thomas (2006) relation for turbulent flow of Bingham material:

$$\sqrt{\frac{8}{f}} = 2.5\log\sqrt{\mathrm{He}} + 2.5\log\left(\sqrt{\theta}\frac{(\theta-1)}{(\theta+1)}\right) + \frac{11.6}{\theta} - \Omega \tag{15}$$

using:

$$\theta = \frac{\tau_w}{\tau_y} = \frac{f\,\rho_m\,u^2}{8\,\tau_y} = \frac{\mathrm{Re}^2\,f}{8\,\mathrm{He}} \tag{16}$$

$$\Omega = -2.5\log\left(\frac{\theta-1}{\theta}\right) - 2.5\frac{\theta+0.5}{\theta^2} \tag{17}$$

where:

θ = the reduced stress variable (-)

Ω = the term accounting for flattening of the velocity near the pipe centre if the local stress does not exceed the yield stress (-). Note the log represents the natural logarithm.

The final friction factor is computed by taking the maximum of the laminar and turbulent friction factor (Equations 14 and 15).

3.2.3 Required power

The required power for transport is a function of the pressure, discharge and the pump efficiency:

$$P = \frac{p\,Q_m}{\eta} \tag{18}$$

where:

P = the power (W)

η = the pump efficiency (-)

p = the pressure (Pa)

Q_m = the mixture discharge (m^3/s).

In computing the pressure, a pipeline length of 1 m is taken. This is effectively taking the hydraulic gradient as the pressure term. For the design of a pump-pipeline system the pump efficiency factor is an important parameter in determining the required power. However, in the examples presented in this paper the pump efficiency is taken as constant.

From the required power, the percentual increase in required power is computed. Since the amount of solids in the computation is constant, the percentual increase in power is also the percentual increase in specific energy consumption of the transport of dry material in W/kg or W/m^3.

4 Possible water savings and energy

For 4 tailings we will compute the possible water and energy savings. It follows a similar approach as Riquelme (2020) to compute the savings. In this paper both laminar and turbulent transport are considered and the effect of a change in pipeline diameter is shown.

4.1 Data

We can distinguish 2 types of data sets. The first one is a sample taken from the underflow of a tailings thickener (van Wijk et al. 2023). The other 3 data sets are tailings which were diluted in the lab to get a yield stress relation with respect to the water to fines ratio. One of these is an in-house sample of mineral sand tailings. The other 2 data sets are from copper ore tailings (Gruszczyński et al. 2019) and a water-clay-sand mixture (van de Ree 2015). Figure 5 shows the yield stress of these data sets compared to the water content to fines ratio defined by Equation 8 as blue dots.

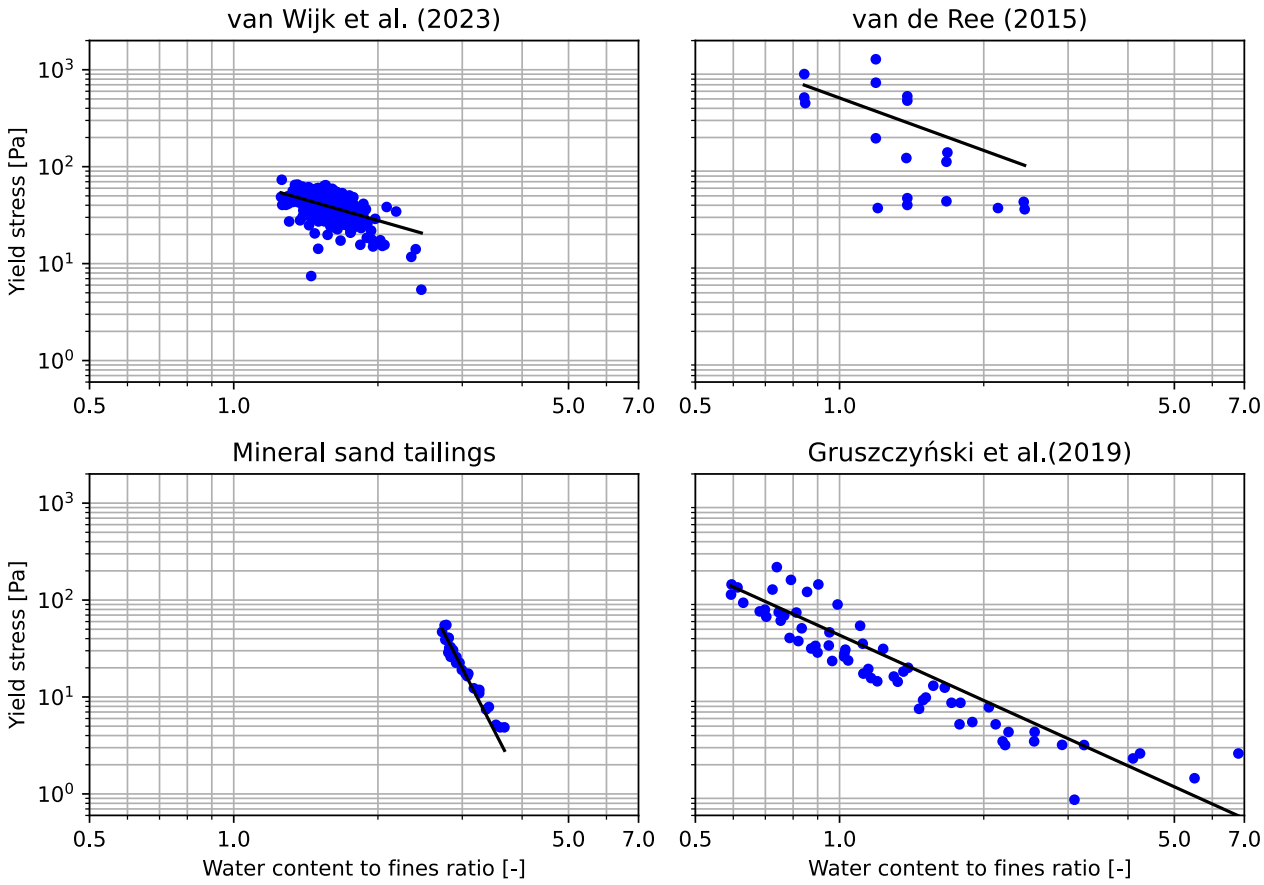

Figure 5 The data from van Wijk et al. (2023), Gruszczyński et al. (2019) and van de Ree (2015) showing the relation between water content to fines ratio and yield stress. The blue dots represent the data points measured using different roto viscometers and the black line is the curve fit of Equation 7

To parameterise the tailings, Equation 7 is fitted through the 4 data sets and is displayed as a black line in Figure 5. Table 1 shows the resulting exponent B. This exponent determines the possible amount of water savings. A lower value means a higher increase in yield stress at the same decrease in water content. The mineral sands have a much lower value of B than the other tailings, meaning an equal percentage of water savings for this tailing will result in a large increase in yield stress. This means only a limited amount of water savings is possible.

The dataset of van Wijk et al. (2023) is taken from the underflow of the tailing's thickener, where a variable and unknown amount of polymers are added to the tailings. Adding polymers will dewater the tailings, creating tailings with a higher density and yield stress. The rake speed in the thickener might have varied, leading to a difference in remoulded state of the tailings.

Table 1 Relation between water content and yield stress (value of exponent B in Equation 7)

Dataset	Exponent B in Equation 7	Concentration (w%) at τ_y = 20Pa	Concentration (w%) at τ_y = 50 Pa	Solid flux turbulent case m³/s
van Wijk et al. (2023)	−1.41	0.4	0.56	0.069
van de Ree (2015)	−1.80	0.21	0.31	0.032
Mineral sand tailings	−9.62	0.36	0.38	0.060
Gruszczyński et al. (2019)	−2.24	0.54	0.64	0.11

4.2 Water savings

The water savings and power usage are computed for laminar and turbulent flow using the data specified in Table 2. In this computation the initial yield stress is 20 Pa, which is increased up to 50 Pa. Table 1 show the mass concentrations for these yield stresses including a sand to fine ratio of 0.65 (Equation 8). This value corresponds to the median of the data of van Wijk et al. (2023). As mentioned, in the computation of the water savings a constant transport of sediment (fines + sand) is assumed for each tailing. While in reality the thickening of tailings results in both a higher yield stress and Bingham plastic viscosity, in this case study only the increase in yield stress is accounted for.

Both a laminar and turbulent case are presented. Most of the tailings are transported in the turbulent regime (near the laminar turbulent transition), since the line speed can be better controlled in the turbulent regime when using centrifugal pumps (Pullum et al. 2018).

Table 2 Parameters used in computing the water savings, hydraulic gradient and power

Heading	Value
Pipe diameter (D)	0.30 m
Bingham viscosity (μ_B)	0.025 Pa s
Yield stress (τ_y)	20–50 Pa
Particle density (ρ_p)	2,700 kg/m³
Sand to fine ratio	0.65
Max. velocity	2.5 m/s, 5.0 m/s

4.2.1 Laminar regime

Figure 6a shows the water savings for the 4 tailings against the yield stress of the mixture. This yield stress is a function of the tailing's density and thus water content to fines ratio. Increasing the yield stress up to 50 Pa

can result in approximately 45% reduction in water usage. Thickening the tailings to get a yield stress of 2.5 times its initial value increase might be unrealistic; however, increasing the yield stress with a marginal 5 Pa, already reduces the water usage by 9.5% for the Gruszczyński et al. (2019) data (red line), which is already a huge amount in arid areas.

Figure 6b shows the hydraulic gradient against the yield stress. Note that the increase in yield stress is a result of the increase in concentration. Since the amount of transported particles is constant, the increase in concentration means a decrease in velocity (Equation 11), which is visualised in Figure 6d. Lastly, the increased power needed for transport is shown in Figure 6c, where it is plotted against the water savings. The 9.5% reduction of water usage for the Gruszczyński et al. (2019) data comes with a 13% increase in required power. The relation between the power increase and the water savings is non-linear, indicating that saving more water will lead to a huge increase in power.

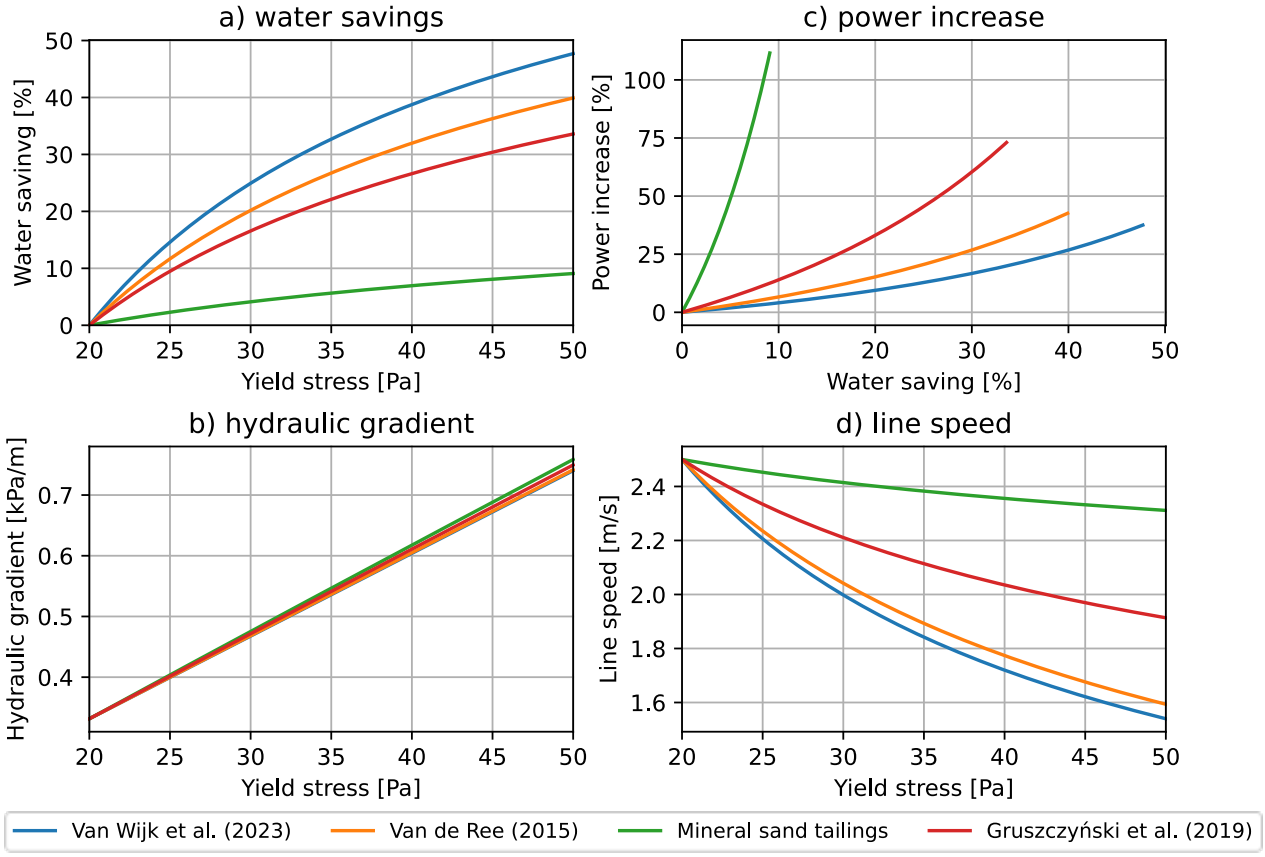

Figure 6 Computed water savings when increasing yield stress for an initial line speed of 2.5 m/s for laminar flow

4.2.2 Turbulent regime

Pullum et al. (2018) showed the need for transporting tailings in the turbulent regime. In the laminar regime small changes in pressure drop lead to large changes in discharge due to the pump pipeline interaction when using centrifugal pumps. In the turbulent regime transport the pressure drop shows a higher increase with increasing discharge. This results in less discharge fluctuations when the pressure drop over the pipe fluctuates due to density and yield stress variations.

When transporting in the turbulent regime, increasing the yield stress of the material results in both water savings and energy reduction. The hydraulic gradient will decrease at increasing yield stress (including the effect of increase in concentration and decreasing velocity). This is visualised in Figure 7b for the lower yield stresses (up to 30 Pa). Increasing the yield stress further leads to a transition to the laminar regime.

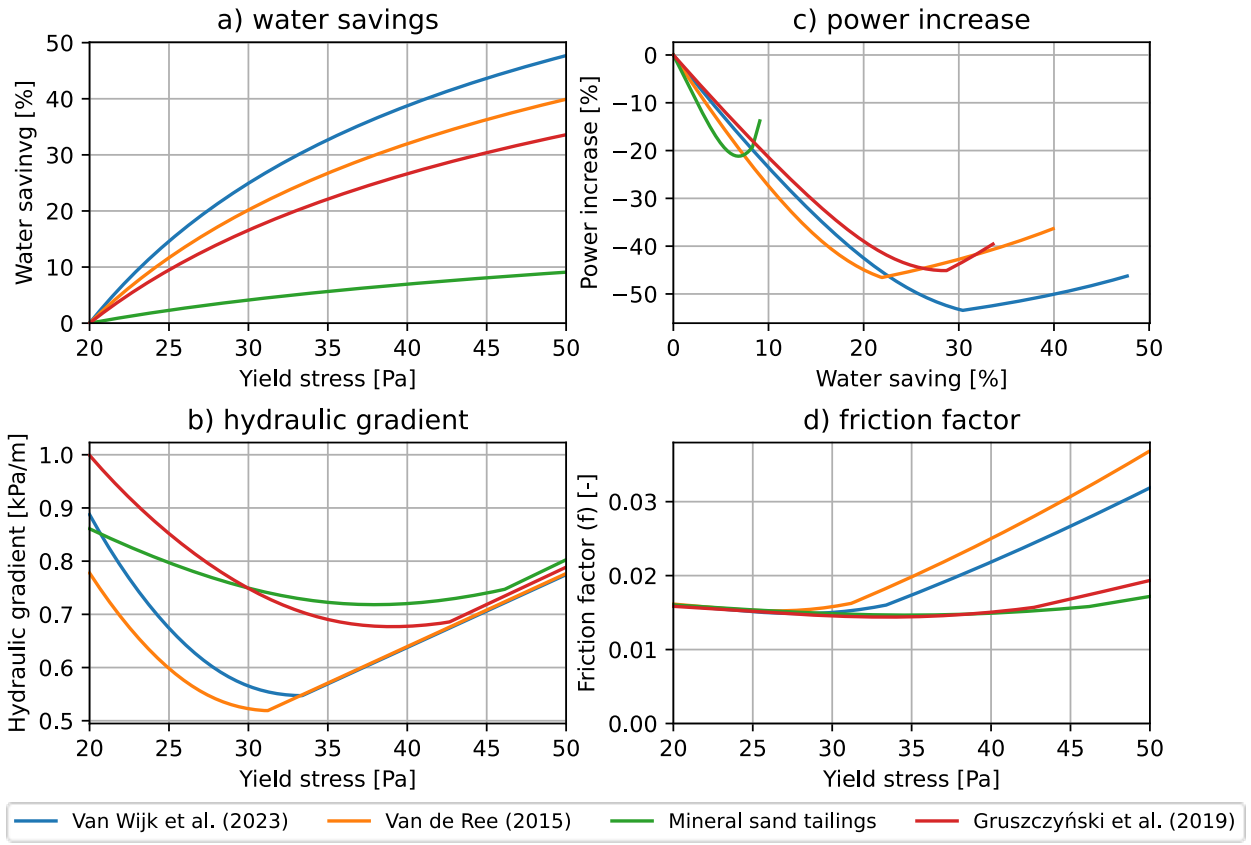

Figure 7 Computed water savings when increasing yield stress for an initial line speed of 5 m/s, for the initial turbulent flow, which changes to laminar flow for higher yield stresses

The friction factor will slightly decrease at increasing yield stress (Figure 7d) in the turbulent regime (located at left of the kink near the minimum in Figure 7d). More pronounced is the decrease in velocity, which was already shown for the laminar case in Figure 6d using a different initial velocity. The reduction of the velocity results in the decrease of the hydraulic gradient. At the transition to the laminar regime, the friction factor increases significantly in relation to the yield stress, therefore the hydraulic gradient also increases. This effect is also mentioned in Pullum et al. (2018) and Sofrá & Boger (2002).

Figure 7a shows the water savings, which are equal to the laminar case, since this only depends on the water content. For the Gruszczyński et al. (2019) data, the 9.5% reduction of water usage leads to a 20% reduction in power consumption (Figure 7c). The transport is still in the turbulent regime.

One can conclude that when operating in the turbulent regime it is always beneficial to increase the concentration and resulting yield stress of the mixture. An upper bound is the point where the pump pressure is not sufficient to transport the tailings or the slurry has a very high solids content.

Increasing the concentration will lead to both a reduction in water usage and energy consumption. However, when the pipeline system is well designed, it does not operate far from the transition point between laminar and turbulent. Lowering the line speed will result in a laminar flow, where the sand fraction in tailings can settle and may form a stagnant bed, possibly forming a blockage. Depending on the properties of the mixture and operational conditions a sliding gelled bed might also occur (Pullum et al. 2010; Talmon et al. 2014). As was mentioned before, a second effect of lowering the line speed is the possibility of a significantly fluctuating discharge due to the small increase in pressure drop at an increase in discharge.

Likely the pipe diameter needs to be changed when optimising the system for more water extraction, since the resulting higher density and yield stress lead to a laminar flow and the risk of laminar flow segregation, leading to a settled bed of solids in the pipeline.

4.2.3 Effect of changing pipe diameter

For the most realistic case we take a well-designed pipeline system with a transport velocity 10% above the laminar turbulent transition velocity. This system uses a 0.3 m pipeline for pumping 20 Pa tailings based on the Gruszczyński et al. (2019) data.

Thickening the slurry at the same solids rate results in a lower transport velocity. A lower transport velocity in this pipe is not possible since we have the risk of operating in the laminar transport regime. Figure 8 shows the effect of changing to a smaller 0.25 m pipe diameter (dashed line) to stay in the turbulent regime. The grey line indicates a transport with a transport velocity higher than a 10% safety margin above the laminar turbulent transition velocity of the new, smaller pipe.

Due to reducing the pipeline inner diameter from 0.3 to 0.25 m, it is possible to thicken the tailings to 73 Pa resulting in 44% water savings. However, at nearly all tailing densities, we do need a significant amount of extra power starting at 163%. Only at the new minimum line speed is there a small reduction in power of 1%.

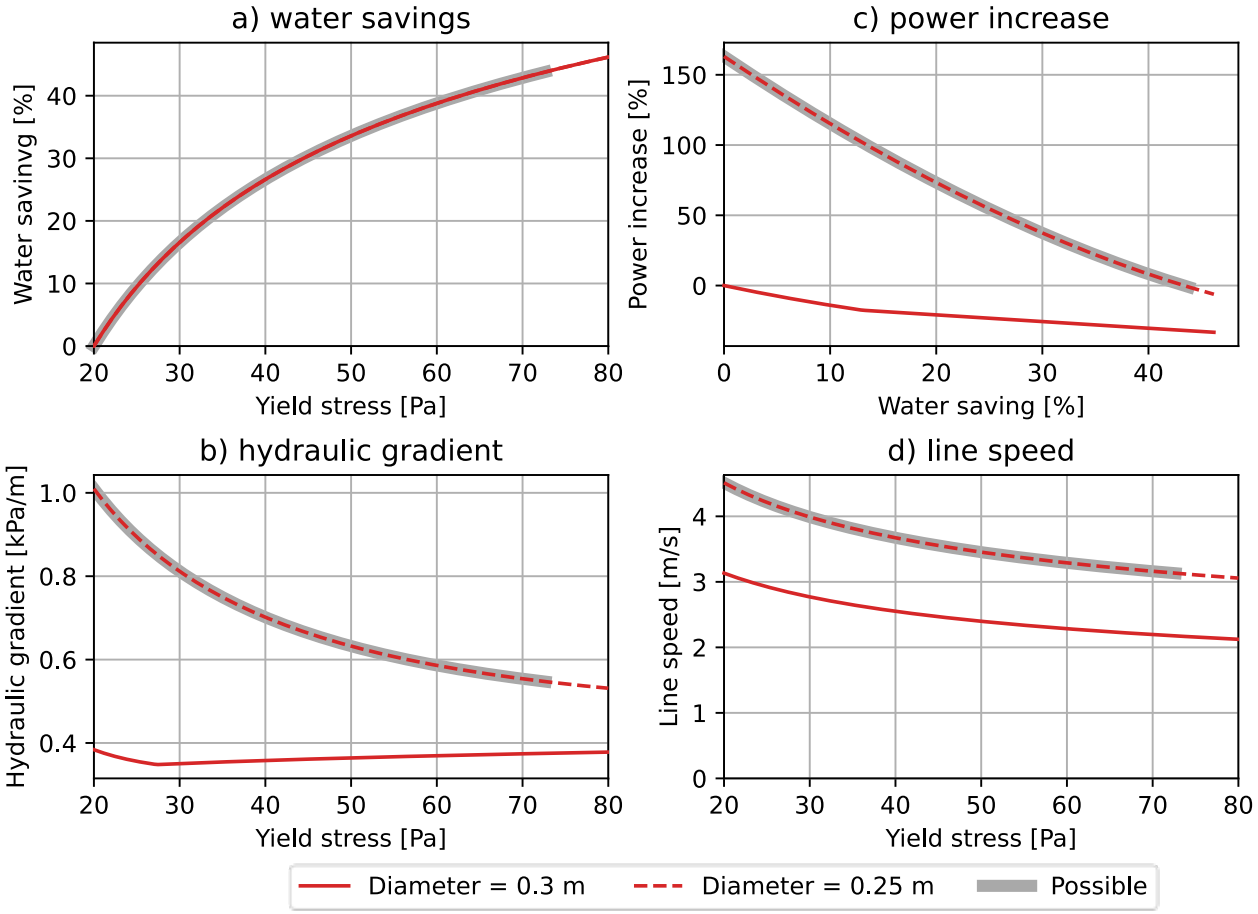

Figure 8 Computed water savings when increasing yield stress for decreasing the pipe diameter for the Gruszczyński et al. (2019) data. The red solid line and dashed line indicates the 0.30 m and 0.25 m diameter pipes, respectively. The grey line indicates the possible line speeds up to a 10% safety margin above the laminar turbulent transition velocity of the smaller pipe

5 Conclusion and outlook

This paper shows the working method of the ARM for measuring the rheology of tailings. It is possible to measure the yield stresses within around 10% from the Haake measurement. The density can also be measured within 10% accuracy. However, measuring the Bingham viscosity is less accurate and has an error around 100%.

A drift in the differential pressure sensors can occur under the influence of changing temperature; however, when pumping tailings from a tailings pond a steady temperature is expected. A drift in the differential sensors is indicated by a difference in density measurement by the 3 U-loops. This indicates that the differential pressure sensors in the U-loops need to be nulled with clear water.

The implementation of ARM technology in mining operations has the potential to drastically reduce water usage. Using a fit function through the data of 4 tailings, we related the water content to fines ratio to the yield stress of the tailings. For the most representative tailings (data from Gruszczyński et al. 2019) this leads to a possible water saving of 9.5% by increasing the yield stress from 20 to 25 Pa. For this increase in yield stress it is still possible to transport in the turbulent regime. Additionally, this reduced the power consumption by 20%. When transporting in the laminar regime, the power consumption would go up with 13% for the specified increase in yield stress.

In a realistic scenario where the line speed is 10% above the laminar-turbulent transition velocity, the line speed cannot be decreased. It is possible to change to a smaller pipe diameter after increasing the density. We presented the example of changing from a 0.3 m to a 0.25 m pipe diameter. Due to this reduction, it is possible to thicken the tailings from 20 to 73 Pa, resulting in 44% water savings.

In this paper we tested the ARM downstream of a tailings thickener to manually guide process adjustments. However, a pilot test campaign in an active mining operation would provide significant additional value. It would allow validation of ARM's performance under true process variability, including changes in particle size, temperature, and flocculant dosing, and quantify the direct economic benefits in terms of reagent savings, energy efficiency, and water recovery.

Deploying the ARM onsite would enable the co-development of automated control loops, linking rheological parameters to flocculant dosing and underflow targets, bringing mining operations closer to fully autonomous thickening systems.

Acknowledgement

The development and validation of the ARM is conducted by Royal IHC, Deltares, Rhosonics Analytical and Sweco Nederland within a Public-Private Partnership: TKI Water Technology. The authors would like to thank the previous researchers on this project: J. van Wijk, M. In 't Veld, J. van der Hoeven and W. Boomsma for their work on the ARM. We are grateful to S. Huisman and M. Busink and S. van Asperen for performing the experiments. We highly appreciate the data provided by A. Kirri. Lastly, we express gratitude to K. Meijer and E. de Hoog for internally reviewing the manuscript.

References

Clift, R & Manning-Clift, DH 1981, 'Continuous measurement of the density of flowing slurries', *International Journal of Multiphase Flow*, vol. 7, no. 5, pp. 555–561.

Chryss, AG, Monch, A & Constanti-Carey, K 2019, 'Online rheology monitoring of a thickener underflow', in AJC Paterson, AB Fourie & D Reid (eds), *Paste 2019: Proceedings of the 22nd International Conference on Paste, Thickened and Filtered Tailings*, Australian Centre for Geomechanics, Perth, pp. 495–504, https://doi.org/10.36487/ACG_rep/1910_37_Chryss

Dodge, DW & Metzner AB, 1959, 'Turbulent flow of non-Newtonian systems', *AlChE Journal*, vol.5, no. 2, pp. 189–204.

Gruszczyński, MF, Błotnicki, J, Czaban, S & Tymiński, T 2019, 'The effect of solid components on the rheological properties of copper ore tailings', Proceedings of the *19th International Conference on Transport and Sedimentation of Solid Particles*, Wrocław University of Environmental and Life Sciences, Wrocław.

Gruszczyński, MF, Kostecki, S, Zieliński, S, Skrzypczak, Z, Stefanek, P, Czaban, S & Popczyk, M 2022, 'A simple and effective method for measuring the density of non-newtonian thickened tailings slurry during hydraulic transport', *Sensors*, vol. 22, no.20.

Jacobs, W, van Kesteren, WGM & Winterwerp, JC 2008, 'Strength of sediment mixtures as a function of sand content and clay mineralogy', *Sediment and Ecohydraulics INTERCOH 2005, Proceedings in Marine Science*, vol. 9, pp. 91–107.

Magnon, E & Cayeux, E 2021, 'Precise method to estimate the Herschel-Bulkley parameters from pipe rheometer measurements', *Fluids*, vol. 6, no. 4.

Pullum, L, Boger & DV, Sofrá, F 2018, 'Hydraulic mineral waste transport and storage, *Annual Review of Fluid Mechanics*, vol. 50, no.1, pp. 157–185.

Pullum, L, Slatter, P, Graham, LJW & Chryss, AG 2010, 'Are tube viscometer data valid for suspension flows?', *Korea-Australia Rheology Journal*, vol. 22, no. 3, pp. 163–168.

Riquelme, C 2020, 'Comparative study of Non-Newtonian thickened tailings in function of water recovered for a specific energy consumption', in H Quelopana (ed.), *Paste 2020: 23rd International Conference on Paste, Thickened and Filtered Tailings*, Gecamin Publications, Santiago, https://doi.org/10.36487/ACG_repo/2052_107

Sofrá, F & Boger, DV 2002, 'Environmental rheology for waste minimisation in the minerals industry', *Chemical Engineering Journal*, vol. 86, no. 3, pp. 319–330.

Sofrà, F & Boger, DV 2011, 'Rheology for thickened tailings and paste — history, state-of-the-art and future directions', in R Jewell & AB Fourie (eds), *Paste 2011: Proceedings of the 14th International Seminar on Paste and Thickened Tailings*, Australian Centre for Geomechanics, Perth, pp. 131–133, https://doi.org/10.36487/ACG_rep/1104_12_Sofra ,

Swamee, PK & Aggarwal, N 2011, 'Explicit equations for laminar flow of Bingham plastic fluids', *Journal of Petroleum Science and Engineering*, vol. 76, no. 3-4, pp. 178–184.

Talmon, AM, Boomsma, W, Nieuwboer, BJ, Rustamov, S, Jaspers, M, van Asperen, S & de Lucas Pardo, M 2024, 'Testing of an autonomous rheometer for optimized tailings thickeners operation', *Proceedings of Tailings and Mine Waste 2024,* Colorado State University, Denver.

Talmon, AM, Hanssen, J, Winterwerp, J, Sittoni, L & van Rhee, C 2016, 'Implementation of tailings rheology in a predictive open-channel beaching model' in Jewell, S Barrera and RJ Jewell (eds), *Paste 2016: Proceedings of the 19th International Seminar on Paste and Thickened Tailings*, Gecamin, Santiago.

Talmon AM, van Kesteren, WGM, Mastbergen, DR, Pennekamp, JGS & Sheets, B 2014, 'Calculation methodology for segregation of solids in non-Newtonian carrier fluids', in D van Zyl, RJ Jewell & AB Fourie (eds), *Paste 2014: Proceedings of the 17th International Seminar on Paste and Thickened Tailings*, InfoMine Inc., Vancouver, pp. 139–153.

van de Ree, THB 2015, *Deposition of High Density Tailings on Beaches*, Master's Thesis, Delft University of Technology, Delft.

van Wijk, JM, Talmon, AM, Meshkati, E, Boomsma, W, van der Hoeven, J, de Jong, S, Hoebe & J, In 't Veld, M 2023, 'Development of a prototype Autonomous RheoMeter for optimized tailings thickeners operations', *Proceedings of the 21st International Hydrotransport Conference*, International Hydrotransport Association, Edmonton.

Wilson, KC & Thomas, AD 2006, 'Analytic model of laminar-turbulent transition for Bingham plastics', *The Canadian Journal of Chemical Engineering*, vol. 84, no. 5, pp. 520–526.

Yusufi, BK, Kapelan Z & Mehta, D 2025, 'Advances in modeling the flow of Herschel–Bulkley fluids in pipes: a review', *Physics of Fluids* vol. 37, no. 2.